International Journal of Applied Earth Observation and Geoinformation 7 (2005) 61–77

INTERNATIONAL JOURNAL OF
APPLIED EARTH OBSERVATION AND GEOINFORMATION

www.elsevier.com/locate/jag

Automated detection and mapping of crown discolouration caused by jack pine budworm with 2.5 m resolution multispectral imagery

Donald G. Leckie *, Ed Cloney, Steve P. Joyce [1]

Canadian Forest Service, Pacific Forestry Centre, Natural Resources Canada, 506 West Burnside Road, Victoria, BC, Canada V8Z 1M5

Received 9 January 2004; accepted 13 December 2004

Abstract

Jack pine budworm (*Choristoneura pinus pinus* (Free.)) is a native insect defoliator of mainly jack pine (*Pinus banksiana* Lamb.) in North America east of the Rocky Mountains. Periodic outbreaks of this insect, which generally last two to three years, can cause growth loss and mortality and have an important impact ecologically and economically in terms of timber production and harvest. The jack pine budworm prefers to feed on current year needles. Their characteristic feeding habits cause discolouration or reddening of the canopy. This red colouration is used to map the distribution and intensity of defoliation that has taken place that year (current defoliation). An accurate and consistent map of the distribution and intensity of budworm defoliation (as represented by the red discolouration) at the stand and within stand level is desirable.

Automated classification of multispectral imagery, such as is available from airborne and new high resolution satellite systems, was explored as a viable tool for objectively classifying current discolouration. Airborne multispectral imagery was acquired at a 2.5 m resolution with the Multispectral Electro-optical Imaging Sensor (MEIS). It recorded imagery in six nadir looking spectral bands specifically designed to detect discolouration caused by budworm and a near-infrared band viewing forward at 35° was also used. A 2200 nm middle infrared image was acquired with a Daedalus scanner. Training and test areas of different levels of discolouration were created based on field observations and a maximum likelihood supervized classification was used to estimate four classes of discolouration (nil-trace, light, moderate and severe). Good discrimination was achieved with an overall accuracy of 84% for the four discolouration levels. The moderate discolouration class was the poorest at 73%, because of confusion with both the severe and light classes. Accuracy on a stand basis was also good, and regional and within stand discolouration patterns were portrayed well. Only three or four well-placed spectral bands were needed for a good classification. A narrow red band, a near-infrared and short wave infrared band were most useful. A forward looking band did not improve discolouration estimation, but further testing is needed to confirm this result.

* Corresponding author. Tel.: +1 250 363 0624; fax: +1 250 363 0775.
E-mail address: dleckie@fc.forestry.ca (D.G. Leckie).

[1] Formerly with the Canadian Forest Service, now with Swedish University of Agricultural Sciences (SLU), Forest Resource Management and Geomatics Section, S-901 83 Umea, Sweden.

doi:10.1016/j.jag.2004.12.002

This method of detecting and classifying discolouration appears to provide a mapping capability useful for conducting jack pine budworm discolouration surveys and integrating this information into decision support systems, forest inventory, growth and yield predictions and the forest management decision-making process.

Keywords: Jack pine budworm; Remote sensing; Spectral bands; Discolouration; Defoliation; Damage assessment

1. Introduction

Outbreaks of forest insect defoliators are a natural and potent influence on forest productivity and timber resources. Innovative improvements to monitoring and managing insect outbreaks are always in demand. Forests in Canada are routinely disturbed and sometimes devastated by insects. Their influence can, in fact, be the single most important factor on forest management of affected regions. For example, during years of peak outbreak of major defoliators, the area affected by moderate and severe defoliation is larger than the total annual area of harvest and forest fires combined for Canada (FIDS, 1980–1995; CFS, 2002). The jack pine budworm (*Choristoneura pinus pinus* (Free.)) can have a serious impact on jack pine (*Pinus banksiana* Lamb.) stands and plantations throughout the range of jack pine in North America (McCullough, 2000). For example, in the mid-1980s jack pine budworm defoliation in Ontario peaked at approximately 3.7 million ha with a resurgence of populations in eastern Ontario beginning in 1992 affecting 420,000 ha (Howse and Meating, 1995). This latter outbreak is the subject of this report. There has not been a recent large outbreak in North America, but because of the cyclical nature of jack pine budworm an outbreak is expected soon.

Accurate mapping of insect presence and damage extent allows forest managers to determine potential effects on wood supply and stand vulnerability, and to design appropriate intervention plans such as reorienting harvest schedules, implementing biological or chemical control programs and conducting salvage logging (MacLean, 1990; Alfaro, 1991; Volney et al., 1995). Various decision support systems have been developed to help manage affected forests, and all require good spatial information on the distribution and levels of budworm damage (McCullough and Marshall, 1993; Power and Gillis, 1995; MacLean and Coulson, 2001).

The jack pine budworm has a similar life history as the eastern spruce budworm (*Choristoneura fumiferana* (Clem.)), a close relative (McCullough, 2000). Eggs are laid on foliage in mid-summer. Neonates hatch within two weeks and seek hibernation sites under bark scales to overwinter. Larvae emerge in the spring and feed first on pollen cones and then on expanding buds and needles of the current year shoots. Most damage, however, occurs in the final instar. At very high population densities, backfeeding may occur on previous-year needles. As the budworm feeds, it produces a protective web or feeding tunnel around the twigs. Partially consumed needles, get caught in this web, dessicate and turn reddish brown. Thus, for a period of time before the wind and rain dislodge these damaged needles from the branches, trees have a reddish colouration. The colouration usually remains for three or four weeks, but peak colouration can be a much shorter period. It normally occurs in early or mid-July. Assessment of the degree of discolouration is used as an estimate of the degree of defoliation for that year, termed current defoliation. Discolouration is the main index used to detect and map the distribution and severity of current year budworm damage.

Traditionally, insect defoliation and discolouration caused by defoliation has been mapped by trained observers using aerial sketch mapping techniques (Heller et al., 1955; Aldrich et al., 1958; Waters et al., 1958; Wert and Roettgering, 1967; Harris and Dawson, 1979; McConnell, 1994; MacLean and MacKinnon, 1996; Ciesla, 2000). Aerial observation can be augmented by airborne video or digital camera data to provide a permanent record of conditions, check and detail mapping, and replace the real-time sketch mapping with office sketch mapping using only the imagery (Leckie and Kneppeck, 1986; Myhre et al., 1990; McConnell, 1994; Knapp and Hoppus, 1996; Ciesla, 2000). Quite a number of factors affect the accuracy and consistency of the maps. These include light conditions, angle of observation, topography, map source into which defoliation is sketched, interpreter training and fatigue, and fragmentation of defoliation pattern. Also, the method's accuracy is compromised by the subjectiveness of human estimation of defoliation or discolouration levels. There is no permanent record or means to recheck results. Presence of non-susceptible forest types and species is often not factored into the mapping and estimates. It is also difficult to map accurately the spatial pattern. Ideally, each forest stand should receive a consistent, detailed evaluation, and there is value in knowing the distribution of different levels of defoliation within stands. This is particularly important for the jack pine budworm defoliation, which is often characterized by a patchy pattern (Nealis et al., 2003).

Multispectral imagery with resolutions in the order of 2–5 m from airborne or satellite platforms may be a viable operational tool for mapping jack pine budworm defoliation. Examination of moderate resolution digital imagery for automatic classification of insect defoliators of conifers in Canada has concentrated mostly on the spruce budworm (Leckie and Gougeon, 1981; Leckie and Ostaff, 1988; Ahern et al., 1991), owing to that insect's wide distribution and economic impact. There have been no moderate resolution studies directly related to mapping the red colouration of current defoliation by the jack pine budworm. Landsat and SPOT satellite imagery with resolutions in the order of 20–30 m have been examined for assessing red stage discolouration (current defoliation) of conifers by several insects (Franklin, 1989 for hemlock looper (*Lambina fiscellaria* (Guen.)); Luther et al., 1991 for black headed budworm (*Acleris variana* (Fren.); Radeloff et al., 1999 for jack pine budworm). Difficulties arise in acquiring imagery during the short temporal window of peak discolouration, from confusion caused by varying stand density, hardwood component and presence of non-susceptible conifer species, and because of the lack of spatial detail (Leckie, 1987; Ekstrand, 1994; Radeloff et al., 1999). Satellite imagery has also been examined for assessment of jack pine budworm top kill (Hall et al., 1995a) and cumulative defoliation or total loss of foliage and mortality (Hopkins et al., 1988). Although symptoms and damage mechanisms are different, several other insect, disease and stressing agents that cause discolouration have also been examined at various resolutions. Examples are: Coops et al. (2003) assessed Dothistroma needle blight in pine, which causes discolouration followed by needle loss, using 10 visible infrared bands, Lawrence and Labus (2003) to detect the red and yellow discolouration caused by the Douglas-fir beetle (*Dendroctonus pseudotsugae*) at the tree level with hyperspectral data, stress in maples (Zarco-Tejada et al., 2002) using imaging spectrometer imagery, root disease symptoms with automated single tree isolation and multispectral classification (Leckie et al., 2004), and several recent studies on assessment of red colouration of pine caused by mountain pine beetle (*Dendroctonus ponderosa*) (Murtha et al., 2000; Franklin et al., 2003; Sakun et al., 2003). A variety of analysis techniques have been used including: maximum likelihood classification, mixture modelling, simple linear regression, discriminant analysis and regression tree, red edge, and spectral derivative methods. Physical based modelling techniques (Hall et al., 1996; Chen and Leblanc, 1997; Stenberg et al., 2003; Tian et al., 2003; Verhoef and Bach, 2003; Wang et al., 2003; Gastellu-Etchegorry et al., 2004) have mostly been applied to extraction of biophysical parameters such as leaf area index (LAI), which can be related to forest damage in terms of loss of foliage and not to the symptom of discolouration.

This paper examines the use of multispectral imagery and the utility of a simple easily applied classification approach for detection and quantification of discolouration caused by the jack pine budworm. Two and a half meter resolution Multispectral Electro-optical Imaging Sensor (MEIS) data was acquired over a test site of varying levels of jack pine budworm discolouration. A short wave infrared band was also acquired by a Daedalus 1260 multispectral scanner (MSS) simultaneously with the MEIS data. The utility of spectral bands specifically optimized for detection of discolouration and the number of spectral bands needed to achieve good discolouration classification were assessed and the benefit of a band viewing forward at 35° from nadir explored. Automated maximum likelihood classification results were compared against sites of known discolouration conditions and results examined in the context of operational implementation in damage assessment surveys.

Imagery was radiometrically corrected for illumination and view angle conditions and then geometrically corrected to cartographic coordinates. Field plots were established and both discolouration and loss of current year's foliage assessed from the ground. Regression of discolouration level versus mean pixel intensity and examination of their statistical separability (Jeffries–Matusita (J–M) distance) were used to assess the best spectral bands and band combinations for discolouration assessment. Maximum likelihood classifications were then tested with several band combinations and number of discolouration classes.

2. Data

2.1. Site

The study area is in eastern Ontario (46°00′N, 77°25′W), near Chalk River approximately 180 km northwest of Ottawa, Ontario. It covers areas occupied by the Canadian Forces Base-Petawawa, Petawawa Research Forest, Algonquin Provincial Park plus surrounding townships. The forest is part of the Great Lakes St. Lawrence forest region (Rowe, 1972) and includes predominantly red pine (*Pinus resinosa* Ait.), white pine (*Pinus strobus* L.), jack pine (*P. banksiana* Lamb.), spruce (*Picea* spp.), aspen (*Populus* spp.), oak (*Quercus* spp.), maple (*Acer* spp.) and birch (*Betula* spp.) in pure and mixed stands. The jack pine stands typically occur on the drier sandy soil sites and stands are often pure, but vary in density and age. The jack pine at the site is near the southern limit of its range.

During 1992, a severe outbreak of jack pine budworm occurred in the region. Although widespread, discolouration was variable among stands and regions within the study area. It ranged from stands that were unaffected through to others with high levels of budworm feeding and strong red discolouration. This pattern was a characteristic of the outbreak (Nealis et al., 2003). In addition, discolouration could also be quite different among trees within the same stand and there was some backfeeding on two year and older needles in some stands. This was the first year of the outbreak in this area, so there was no defoliation or exposure of bare branches caused by budworm activity from previous years. Only the jack pine was affected, other species were not attacked.

2.2. Remote sensing data

Airborne Multispectral Electro-optical Imaging Sensor (MEIS II) (McColl et al., 1984) and Daedulus Model 1260 airborne multispectral scanner (Zwick et al., 1980) data were recorded for two flight lines on July 21, 1992, between 1001 and 1019 h EDT. Discolouration of the defoliated trees had reached its peak about a week earlier, but was still intense. Imagery was acquired from an aircraft flown at approximately 3600 m above ground level giving across track instantaneous field of views on the ground of 2.5 m for the MEIS nadir imagery, 3.0 m for the MEIS stereo channels and 9.0 m for the airborne MSS data. The sampling interval for the two sensors resulted in along track pixel spacings of 1.6 m for the MEIS sensor and 3.3 m for the Daedalus MSS. Across track pixel spacing of the MEIS was the same as the instantaneous field of view, but for the Daedalus scanner the across track sampling interval was 5.3 m. Flight lines were 30 km long and the swath width of the MEIS was 2.6 km. Normal colour photographs (Kodak Aerocolor Negative 2445) at a scale of 1:23,500 were acquired simultaneously. One flight line was oriented approximately east to west (azimuth 258°) while the second was nearly perpendicular to the first at an azimuth of 148°. Weather was clear except for one small cloud. Sun elevation and azimuth were 48° and 113°, respectively.

MEIS imagery was acquired in six nadir viewing bands and two infrared stereo bands (i.e., bands viewing fore and aft of the aircraft at 35°). This band set (Table 1) was specifically designed by the authors for spruce budworm, this study and other damage assessment applications. The nadir bands were optimized for detecting spruce budworm discolouration (current defoliation) symptoms (Leckie et al., 1988), which have similar characteristics as jack pine budworm defoliation. The off-nadir bands are designed to test a hypothesis that viewing the canopy at an angle versus nadir may give better discrimination of discolouration since at an angle the sensor is mainly viewing the canopy and discolouration is often greatest on the upper crown of attacked trees (Cerezke, 1986; Moody, 1986). At nadir, a sensor is viewing the

Table 1
Spectral bands used in this study[a] and correlation coefficients of determination (R^2-values) for regressions of discolouration index vs. mean band intensity for sample areas

Sensor	Band number	Wavelength midpoint (nm)	Bandwidth (nm)	R^2-value
MEIS	1	448	30	0.08
MEIS	2	525	10	0.31
MEIS	3	553	14	0.27
MEIS	4	593	13	0.64
MEIS	5	667	15	0.88
MEIS	6	780	33	0.92
MEIS	7 (stereo fore)	780	33	0.71
MSS	8	2200	120	0.60

[a] In this study, an additional MEIS aft-looking stereo channel at 875 nm was acquired but not used.

trees and often the ground between them and this can cause confusion in classifying damage. The MEIS sensor does not operate in the short wave infrared, therefore Daedalus airborne MSS data in a 2200 nm band were acquired on the same aircraft simultaneously with the MEIS imagery.

The image data was calibrated such that digital value represented at sensor radiance but scaled to give an image intensity between 0 and 255. No atmospheric correction or conversion to reflectance values was conducted. Imagery was corrected for radiometric variations across the image due to the atmosphere and illumination-view angle effects. A well-established empirical approach was used (Leckie, 1987; Reinartz et al., 1988; Ahern et al., 1991; Danson and Curran, 1991; Leckie et al., 1996, 2004). Sample areas of dense mature red pine were acquired across the image and signatures calculated. For each spectral band, a second order polynomial correction curve was fit to the mean intensity value of the red pine areas versus the distance (pixel columns) from nadir to the center of the sample areas. An additive offset was then applied to the intensity of the pixels of each column of the imagery. The offset for each pixel of a column is taken to be equal to the number of intensity levels the curve at that column is above or below the intensity level of the curve at nadir. A similar best fit polynomial of the red pine sample areas after correction will result in a straight-line of slope zero (i.e., no systematic radiometric variation across the image). Sample areas of jack pine would have been used but there was not a sufficient distribution of stands of similar density, discolouration condition and age class across the image. The two flight lines were then radiometrically normalized. The common area where the two flight lines intersect was checked for differences in the mean image values of each band and an additive offset was applied to the pixel values of each band of the north–south flight line such that the resulting means of the two images in the overlap area were the same.

After radiometric correction, the data were geometrically corrected to UTM coordinates. This was done using the method of Gibson et al. (1994), which incorporates attitude and velocity information from an inertial navigation system and ground control points of known x, y and z coordinates. The geometric correction was applied to the nadir MEIS, stereo MEIS and airborne MSS middle infrared channel. Resulting imagery was 2 m in resolution. A cubic convolution resampling kernel was used. Fig. 1 gives an example of a section of the corrected imagery.

2.3. Description and estimation of discolouration

Aerial visual observation and oblique 35 mm colour photography was conducted at the same time as the acquisition of the airborne imagery. Aerial reconnaissance was also conducted from ultralight and fixed wing aircraft in the weeks previous to the flights in order to design the flight lines. These were during the time of peak discolouration. These aerial observations, those on the day of the flight, the oblique aerial photographs and forest inventory were all used to select sites of varying discolouration levels, densities, ages and stand compositions. Sixty-seven ground observation sites were visited and assessed on

Fig. 1. Segment of the imagery used in the study. The 667, 553 and 448 nm bands are displayed as red, green and blue. The segment is 6.0 km by 2.3 km. (For interpretation of the references to colour in this figure legend, the reader is referred to the web version of this article.)

the ground. Additional aerial observation sites were assessed using only the aerial observation and oblique photographs. Sites were chosen to represent approximately equal numbers of the different discolouration conditions plus stand densities, ages and compositions in a proportion representative of the study area landscape. On all sites the amount of red colouration was assessed and assigned to four classes of discolouration: nil or trace, light, moderate and severe. The degree of redness corresponds to the amount of foliage eaten by the budworm and these classes correspond to overall current year defoliation (needle loss) levels of <10, 11–30, 31–65 and 66–100%, respectively. The classes follow closely those routinely used for jack pine budworm damage assessment (Hall et al., 1995b).

Ground based assessments were made on 67 sites, defined as contiguous areas of fairly uniform defoliation and discolouration, usually 5–12 ha in size. Binoculars were used to examine individual crowns in detail. After a thorough walk through, one of the discolouration classes was chosen to represent the entire site. Other measurements were also taken at the same time. A numerical "redness value" was estimated (1–10), based on whether redness was absent, lightly apparent, moderately apparent or very apparent. Current defoliation level was calculated for each site by estimating the percent of trees in the site at each current defoliation level. For instance, if a site was considered to have 80% of its trees having moderate defoliation, with an average defoliation of current growth estimated at 50% and the remaining 20% of the trees being unaffected, then a value of 40 would be calculated ($80 \times 0.5 + 20 \times 0.0$). This is directly related to the amount of red discolouration and is termed "discolouration index". Age of the stands was determined through analysis of increment cores and crown closure was visually estimated in 10% classes. Site assessment was completed by photographing representative trees. The site boundary was then drawn on airphotos for later reference.

An independent ground assessment of a sample of sites was conducted in August after the damaged foliage had fallen and red colouration had disappeared. The damage assessment was done by the forest health officer responsible for monitoring the region where the outbreak occurred. He independently assessed 26 of the 67 ground sites by estimating overall current defoliation level using binoculars, in the same manner as was previously done. For eight of the sites, a detailed assessment was carried out by removing a 60 cm branch tip from the mid-crown of six representative trees in each site. On each branch an estimate of defoliation was made by visually dividing the branch into quarters and examining all branchlets, keeping a running total of the percent defoliation and computing a final overall percentage for the branch. The average percent defoliation of the six branches of a site was used to assign the stand to a current defoliation level and discolouration class. Overall agreement of the two independent surveys was good with only two sites being assigned to different classes.

2.4. Sample areas

From the ground and aerial observation sites, sample areas were selected for use in characterizing the spectral signature of different discolouration conditions, for training the maximum likelihood classifier and for independent testing of the accuracy of the classification. These sample areas were chosen to match the location of ground observation sites or areas of clearly defined discolouration levels based on oblique aerial photographs and aerial observation. Fifty-one areas were delineated on the imagery. They evenly represent the range of discolouration conditions from unaffected through to very severely discoloured stands and were also selected to be distributed spatially over the length and width of each of the two flight lines. Each sample area was then allocated to one of the four discolouration classes: nil-trace, light, moderate and severe. The jack pine stands used in this study were dense (most 65–75% crown closure but ranging from 50 to 90%) and between the ages of 30 and 65 years, with a few younger stands down to 20 years old. Most sites were pure jack pine, but some had minor components of other species, usually white pine. The individual training and test areas were typically between 300 and 1800 pixels (i.e., 6–36 ha) in size. In addition to unaffected jack pine and budworm attacked jack pine areas, sample areas of a non-jack pine coniferous class were delineated and consisted of mainly white pine.

Individual sample areas were randomly assigned to either training or test sets such that 17 sample areas were designated for training and 34 for testing. The individual training sample areas of each class were amalgamated and used to generate the signatures that represent each class and the test areas were utilized to estimate the accuracy of the classification. The process resulted in a set of approximately 10–12 sample areas of each discolouration class distributed across the study site, approximately 1/3 used for training and 2/3 for testing.

3. Analysis and results

3.1. Examination of the utility of spectral bands

3.1.1. Regression analysis

The relationship of individual bands to discolouration level provides insight into the usefulness of the bands for separating discolouration classes. Empirical polynomial fit and coefficients of determination were used to provide insight into the influence of discolouration on the spectral response in each band and the effectiveness of the band for discriminating discolouration levels. Multiple regressions were also conducted to help determine the effectiveness of multiple bands in combination. Half the sample areas (26) were used as input into a regression analysis. For each sample area, "discolouration index" as determined from the field observations was plotted against mean image intensity in each band. For the spectral bands with good relationships between discolouration and intensity, the relationship was generally curvilinear with greater change in image intensity with discolouration at low discolouration levels (Fig. 2). However, if only data above discolouration index 15 were considered, the relationship was close to a straight-line.

Second-degree polynomial regressions ($a + bx + cx^2$) of discolouration index (dependent variable) and image mean intensity (independent variable) were determined for the six nadir bands, the stereo channel and airborne MSS short wave infrared band (Table 1). The near-infrared band (780 nm) and red band (667 nm) had highest correlation coefficient of determination (R^2) values, followed by the stereo near-infrared band. The blue and green bands (448, 553 and 525 nm bands) had weak relationships of band intensity to discolouration. The 2200 nm band had only a moderate relationship with discolouration; this may be in part due to its lower original acquisition resolution. Fig. 2 gives examples of the regressions.

A multiple linear regression model of all eight bands combined (six nadir, stereo fore and airborne MSS SWIR band), resulted in an R^2-value of 0.942. This is not much higher than the 780 nm band by itself. Multiple regressions with all six nadir channels produced an R^2 of 0.938. R^2-values for combinations of the 667, 780 nm, stereo and 2200 nm bands, the 667, 780 nm and stereo bands, and only the 667 and 780 nm bands were 0.904, 0.900 and 0.892, respectively. Root

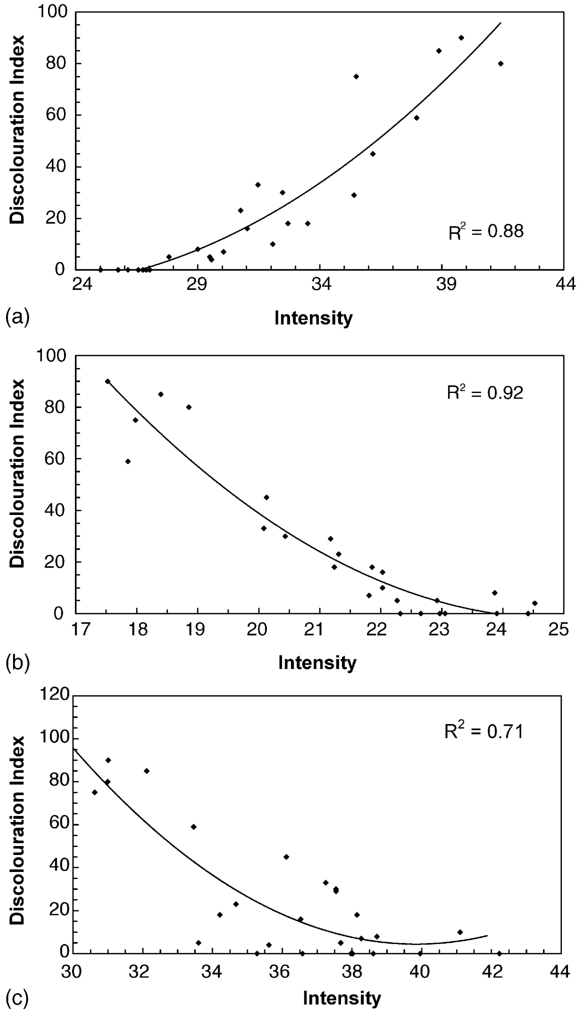

Fig. 2. Discolouration index vs. mean band intensity for sample areas. The second order polynomial regression curve is also given: (a) 667 nm band; (b) 780 nm band; (c) 780 nm stereo forward viewing band.

mean square error for a two band regression (the 667 and 780 nm bands) was 10.1, 8.4 for all six nadir bands and approximately 8.5 for regressions when the stereo and short wave infrared band were added. It is clear that only one or two bands are needed to produce a strong regression relationship.

3.1.2. Discolouration class separability analysis

Jeffries–Matusita distance (Richards, 1993), a statistical measure of the separabilities of two classes, was used to determine the best combinations of bands for separating the discolouration classes (nil-trace, light, moderate and severe) from each other and from the non-jack pine coniferous class. Separability using a set of bands was determined using the spectral signature (mean and covariance matrix) of the training areas of each class. J–M distance ranges from 0 to 2.0 with higher values representing better separability of class pairs. Therefore, the bands or band combinations producing the highest J–M distance averaged over each pair of discolouration classes can be considered the best for discriminating discolouration levels. The best single band for separating classes was taken to be that band producing the largest average J–M distance between each possible pair of classes. The best combination of two bands was determined using the best single band in combination with each of the remaining bands (the combination with the largest average J–M distance is used to indicate the best sequential band combination). A similar procedure was followed for combinations of three to eight bands (Table 2).

For separating the nil-trace, light, moderate and severe classes, the best single bands were the 667 and 2200 nm bands, followed with considerably less separability by the near-infrared bands (nadir and stereo and the 593 nm band). The 553, 525 and 448 nm bands had low J–M distances (Table 2). The best sequential combination of two bands was the 667 and 780 nm band, with the 2200 nm airborne MSS band being added to these for the best sequential combination of three bands. There is a large increase in separability for two bands versus one band and smaller increases with each additional band thereafter. The best single bands, as well as, combinations of bands were similar if the J–M distances for only the light, moderate and severe classes were considered. The order of entry into the combination of best bands if only the six nadir bands were included (as might be the case for sensor systems that do not have a short wave infrared or forward looking capability) was the 667, 780, 448, 553, 593 and 525 nm bands.

When separability of the non-jack pine conifer class was included in the analysis along with the four jack pine classes (data not shown), the two near-infrared bands (nadir and stereo) became the most important single bands. The stereo 780 nm band, 667 nm band, 780 nm nadir band and 2200 nm band are the sequence of best four bands in combination

Table 2
J–M distance for the sequence of best one to eight bands

Best band combinations (band central wavelength, nm)	Band (central wavelength, nm) Jeffries–Matusita distance							
Single bands	667	2200	780	780 fore	593	553	525	448
	0.798	0.618	0.339	0.302	0.296	0.176	0.171	0.123
Two bands—667 with		780	448	553	780 fore	525	2200	593
		1.281	1.117	1.064	0.983	0.977	0.949	0.885
Three bands—667, 780 with			2200	448	780 fore	553	593	525
			1.376	1.329	1.324	1.318	1.313	1.305
Four bands—667, 780, 2200 with				448	780 fore	593	553	525
				1.424	1.413	1.405	1.405	1.393
Five bands—667, 780, 2200, 448 with					553	780 fore	525	593
					1.464	1.459	1.457	1.456
Six bands—667, 780, 2200, 448, 553 with						780 fore	525	593
						1.492	1.491	1.490
Seven bands—667, 780, 2200, 448, 553, 780 fore with							593	525
							1.522	1.521
Eight bands—667, 780, 2200, 448, 553, 780 fore, 593 with								525
								1.551

The J–M distance is the average over each pair of classes among the four discolouration classes (healthy, light, moderate and severe).

with each other (based on the average J–M distance for the healthy, light, moderate and severe discolouration classes plus the non-jack pine conifer class). For the non-jack pine conifer class versus each of the other four classes the best single band was the stereo 780 nm channel, followed by the nadir 780 nm band (average J–M distances of 1.61 and 1.55, respectively). The 448 and 553 nm bands were the next most important single bands (J–M distance of 0.97 and 0.91, respectively). It is interesting to note that the best single bands for separating healthy jack pine from non-jack pine conifer were the same as for separating non-jack pine conifer from defoliated jack pine. Therefore, a near-infrared band was useful not only for separating discolouration classes but also for separating jack pine from other conifers (in this case, mostly white pine).

3.2. Classification of discolouration classes

Maximum likelihood classifications (Richards, 1993) were conducted with different numbers of bands based on the band combinations determined in the separability analysis. The spectral signatures of the training areas of each class were used as input to the classification. The resulting classifications were smoothed to remove isolated pixels or small clusters of one class contained within another larger class. Smoothing is accomplished with a post-classification filtering algorithm that eliminates areas of 10 pixels or less of the same class (10 pixels connected in any orientation including diagonally). Pixels in these small areas are assigned the class of adjacent areas through a process of erosion of the boundary. This smoothing results in a better representation of discolouration as it would be mapped operationally, and better accuracies.

With current sketch map and ground survey techniques, discolouration is generally mapped in large units assigned to a single representative class. The true situation within a stand is that there is often a mix of discolouration levels within zones or even among adjacent trees. The ground truth class assigned to training and test areas is an average class, the area itself having some variation in level within it. Therefore, the smoothing applied to the classification helps make the image derived classes for the area more compatible with that described from the ground (ground truth). Classification accuracies were determined by comparing the classification of each pixel in the test areas to the categorization of that test area as determined on the ground. Classifications included the nil-trace jack pine class, the light, moderate and severe discolouration classes plus the non-jack pine conifer

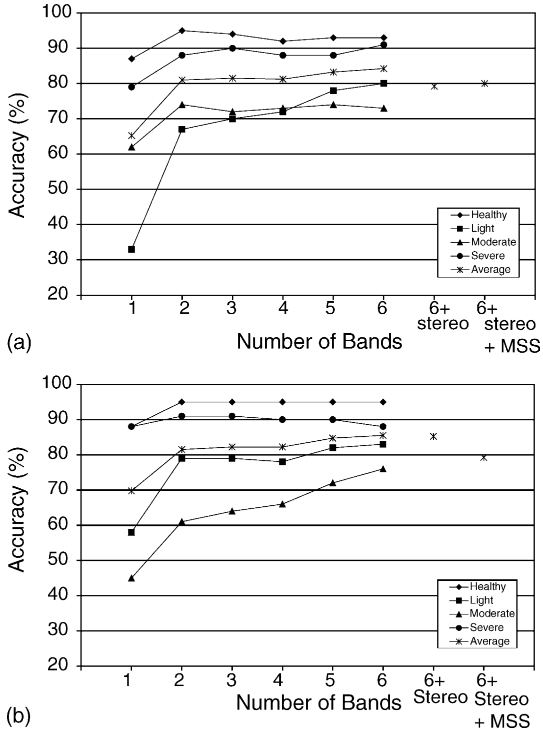

Fig. 3. Average classification accuracy for the four discolouration classes vs. number of nadir bands used. Also given are the accuracies when the stereo and 2200 nm bands were added. The average accuracy is the mean of the healthy, light, moderate and severe class accuracies. (a) Omission accuracy (percent pixels of test areas of each class classified correctly). (b) Commission accuracy (percent of all pixels within the test areas classified as a class that are actually of that class).

class. The latter class was included in order to prevent areas of other conifers being incorrectly classified as jack pine or discolouration.

Fig. 3 plots the classification accuracy of discolouration for classifications with the best combination of different numbers of bands as specified by the J–M distance analysis (Table 2). It appears that only two or three bands are needed to produce good accuracies. However, if one examines omission errors for the light class and commission errors for the light and moderate classes, there is an approximate 5% increase in accuracy for classifications using the best four versus five bands. Maximum overall classification accuracies were in the order of 85% (Fig. 3, average accuracy of the four discolouration classes).

Table 3 gives the confusion matrix for a classification of four discolouration levels using all six nadir bands. Fig. 4 shows the corresponding classified image for a segment of the test area. Regional patterns of discolouration and within stand variations are evident. Omission accuracy was 93, 80, 73 and 91%, respectively, for the nil, light, moderate and severe classes. This represents the number of pixels in the test areas of each class actually classified as that class. Average accuracy over the four classes was 84%. Trends observable in both Table 3 and Fig. 4 are common to other band combinations. Confusion was between adjacent classes. The moderate class was most poorly classified, having significant misclassification with both the light and severe classes. Accuracy of a classification without post-classification smoothing was in the order of 5–10% lower at 89, 70, 65 and 86% for nil, light, moderate and severe, respectively. Commission accuracy averaged over each discolouration class was 86% (95, 83, 76 and 88%, respectively, for nil to severe). It represents the percent of all pixels in the test areas classified as a class that were actually that class (i.e., were in the test area of that class). It must be remembered that there can be a mix of discolouration levels within the test areas and the above analysis assumes all pixels are the discolouration class assigned to the site.

Table 3
Confusion matrix for classification of the six nadir bands for classes of healthy jack pine, light, moderate and severe discolouration and a class of non-jack pine conifer giving the percent of pixels in the test areas of each discolouration class classified as each class

Ground truth	Classification						
	Healthy	Light	Moderate	Severe	Non-jack pine conifer	Unclassified	Total no. of pixels
Healthy	92.7	4.5	0	0	2.8	0	12426
Light	6.0	80.0	9.9	3.5	0.6	0	8996
Moderate	0.1	14.0	73.3	12.1	0.0	0.5	6315
Severe	0	1.0	6.2	90.5	0.0	2.3	8529

Also provided is the total number of pixels in the test areas.

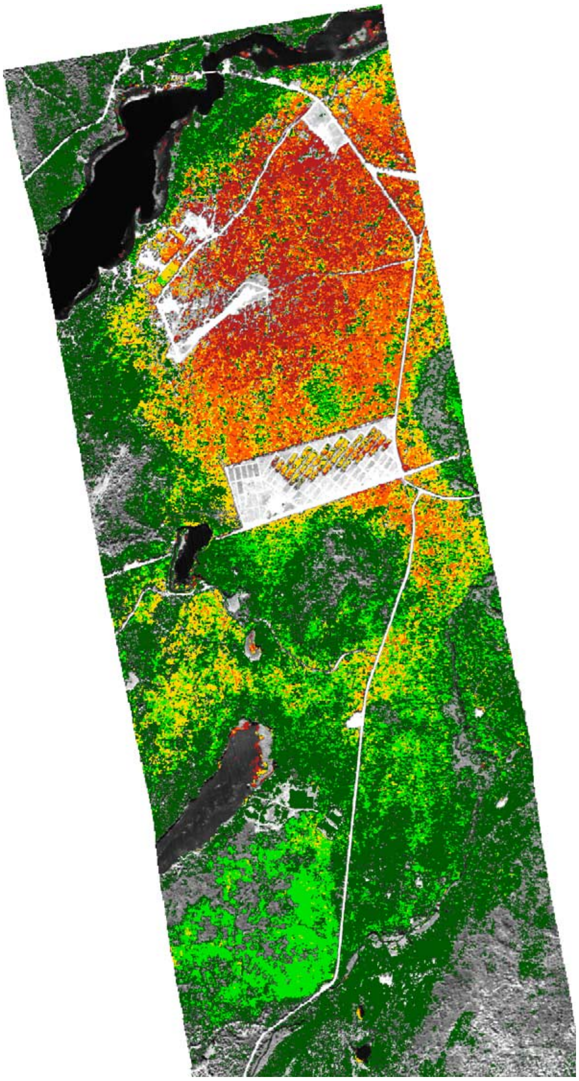

Fig. 4. Classified image for the segment shown in Fig. 1. Classification is with all six nadir bands overlaid on the 553 nm image. Healthy: light green, light: yellow, moderate: orange, severe: red, non-jack pine conifer: dark green. (For interpretation of the references to colour in this figure legend, the reader is referred to the web version of this article.)

Accuracy was very good when assessed on a site basis (i.e., if the whole sample area was assigned to one class based on the proportion of pixels within the site classified as each discolouration class). A discolouration index was assigned to each site in a similar fashion as was done using the field data. The percent of pixels of each class in the test sample area was multiplied by the midpoint percent of the class (0.05 for nil-trace, 0.20 for light, 0.425 for moderate and 0.825 for severe). These were summed over the four classes to give a discolouration index. Using this procedure, all sample areas were assigned to the correct class. If test areas were assigned to the class of the most commonly occurring discolouration class within it, then all but one test area, a moderate site, was correctly labelled.

Non-jack pine conifer areas had few pixels (<1%) classified as light, moderate or severe discolouration. It can also be seen from Fig. 4 that there were few spurious pixels or surface types (unrelated to jack pine or discolouration) that were classified as discolouration. For example, classification results (six nadir bands) were analyzed for a large image segment representative of non-jack pine forest land (i.e., a typical area of other forest types, wetlands, water, roads and other surface types). Only 2.4% of the pixels in this area were classified as one of the discolouration classes (light, moderate or severe). Most error was associated with shallow water, wetland and stand edges where shadows occur. If a water class was included in the classification, the error was approximately 1%. This error increased but remained low even when only two or three spectral bands were used in the classification (2.7% with a water class and 5.1% without a water class). In addition, in operational surveys results will likely be overlain on the forest inventory so that only jack pine stands would be considered and misclassification of other surface and forest types as discolouration would not be a problem.

Despite being important spectral bands in the separability analysis, the addition of the stereo and short wave infrared bands to the six nadir bands did not result in gains over using only the six nadir bands. Addition of the stereo band gave similar average overall accuracies of the discolouration classes, but a shift in classification of pixels towards less defoliated classes. Also, the amount of non-defoliated jack pine misclassified as non-jack pine conifer rose from 2 to 18%. Replacement of band six (nadir near-infrared band) with the equivalent stereo infrared band resulted in similar affects. Addition of the 2200 nm band to the six nadir bands resulted in only small changes in both the classification accuracies of each class, and in the overall accuracy.

4. Discussion

The MEIS imagery using specialized spectral bands was successful in classifying jack pine budworm discolouration to a degree of accuracy that meets operational requirements for defoliation and discolouration assessment (Volney et al., 1995; MacLean and MacKinnon, 1996; Ciesla, 2000). Four discolouration levels were accurately classified (nil-trace, light, moderate and severe). Discolouration was determined to within one discolouration class 97% of the time for the healthy test pixels, 96% of the time for light test areas, 99% for the moderate class and 97% for severe discolouration. Accuracy for the exact class was also high. The most distinctive classes were the extreme classes, nil-trace and severe, with accuracies of 93 and 91%, respectively. The accuracy of the light class was less at 80%. Accuracy of the moderate class was 73%. There was considerable confusion of areas of moderate discolouration with both the severe and light classes. This also occurs in the ocular assessment of defoliation and discolouration on the ground or from aerial observation (Volney, 1988). If sites were assigned to a single discolouration class based on the proportion of pixels of each class within them, accuracy on a site basis was very good. Regression analysis indicated that discolouration level (index) of a pixel can be estimated to within a RMS error of 10 using the 667 and 780 nm digital values for that pixel (8.4 using all 6 nadir bands). It must be remembered that discolouration occurs in a continuum of levels and, in the case of jack pine budworm, can be variable within stands and even between adjacent trees.

It has also been shown that good accuracy is achievable with a minimum number of spectral bands, if they are well chosen. The spectral bands of the MEIS spruce budworm stereo filter set, specifically designed to detect current spruce budworm discolouration, proved to also be effective for assessing jack pine budworm discolouration. In order to confirm the effectiveness of the bands and relate them to the physical characteristics of the tree components and damage symptoms, findings for this study are compared to those of the ground based studies of discolouration of trees (Leckie et al., 1988) and known spectral characteristics of the needles, red feeding debris and branches (Leckie et al., 1989) related to spruce budworm. The narrow red band at 667 nm was the best band for detecting discolouration of spruce budworm and as indicated in this study also for jack pine budworm. The red colouration is caused by dried needles, frass (larval excrement) and other feeding debris, and is also enhanced by exposure of bare twigs. The MEIS data of this study were acquired after peak colouration and the importance of this band and indeed classification accuracy would be expected to be even greater at maximum colouration. The near-infrared (780 nm) band was also very important for discriminating discolouration level. A decrease in near-infrared reflectance with increasing discolouration is a manifestation of loss of healthy foliage (with its high near-infrared reflectance), exposure of bark (with lower near-infrared reflectance) and presence of red feeding debris (also with low near-infrared reflectance) (Leckie et al., 1989). The green and blue bands in general are useful for discriminating forest types, and in this study had low value for discriminating discolouration levels. This is in keeping with spectral characteristics determined for spruce budworm, which showed only a weak relationship of the blue and green part of the spectrum to discolouration. The blue part of the spectrum, however, is noted to be useful for detecting loss of foliage and tree mortality through exposure of branches. Weathered branches also often have high blue reflectance. The test site had only suffered one year of budworm feeding and exposure and weathering of branches and the importance of the blue band were not strong in this data set, although in the sequence of best bands the 448 nm band entered as the fourth band after the red, near-infrared and short wave infrared bands. Jack pine budworm defoliation generally only occurs over two or three years in succession and therefore exposure and subsequent weathering of branches may not be as strong as in spruce budworm defoliation, which often has many years of defoliation. As mortality occurs, it would be expected that a blue spectral band would become more useful for detection of jack pine budworm damage. The narrow spectral band near 525 nm had shown in ground based spectral studies better capabilities than surrounding wavelengths for detecting current spruce budworm discolouration. Results of this study, however, showed it to be poor at differentiating levels of jack pine discolouration. The 590 nm band, according to the spectrometer data, is in a region of little change of reflectance with increasing discolouration and is at a transition from decreasing reflectance with discolouration in the green part of the spectrum to increasing reflectance in the red. The MEIS data showed it had moderate capability for discriminating jack pine budworm discolouration as a single band, but was one of the last bands to enter into the sequence of best combinations of bands.

The 2200 nm short wave band was also useful for discolouration assessment. Short wave bands have consistently proved effective in detecting loss of foliage and exposure of branches (Leckie and Gougeon, 1981; Ekstrand, 1990; Franklin et al., 1995; Hall et al., 1995a). The spectrometer study of Leckie et al. (1988) regarding discolouration caused by the spruce budworm indicated the short wave infrared regions (1440–1810 and 1960–2400 nm) to be better than visible and near-infrared bands for discrimination and a specific spectral region from 2030 to 2210 nm had the greatest discrimination capability of all wavelengths. Despite the short wave data of this study being acquired at lower resolution than the MEIS bands, the 2200 nm band was the second most important single band for discolouration discrimination and entered third in the sequence of best bands. Although the short wave infrared band did not improve accuracies when added to the six nadir bands, it is recommended that, if feasible, a short wave infrared band should be included in any sensor configuration utilized for jack pine budworm discolouration assessment.

Since budworm feeding and consequent discolouration is often more intense in the upper crown of trees and viewing at an angle may reduce confusion caused by density variation and viewing of the ground or understory, it was hypothesized that if the sensor bands were oriented to view the forest at an angle (e.g., forward viewing), discolouration assessment would be more accurate. In addition to the MEIS sensor, there are a number of imagers both airborne and spaceborne available that can acquire spectral data at different angles (e.g., Advanced Solid-State Array Spectroradiometer (ASAS), Irons et al., 1991; Frequent Image-Frames Enhanced Digital Ortho-Rectified Mapping (FIFEDOM), Wehn et al., 2002; Advanced Digital Sensor (ADS40), Sandau et al., 2000; POLarizarion and Directionality of Earth Reflectances (airPOLDER and POLDER), Deschamps et al., 1994; Multi-angle Imaging SpectroRadiometer (airMISR and MISR), Diner et al., 1998a,b; Compact High Resolution Imaging Spectrometer (CHRIS), BNCS, 2002). In addition, several optical satellite sensors are pointable, including the high resolution IKONOS and Quickbird systems, thus permitting acquisition of data at an angle. Angular data has been shown to be useful for estimating biophysical parameters and for land cover typing (e.g., Leroy and Bréon, 1996; Diner et al., 1999; Gemmel and McDonald, 2000; Chen et al., 2002; Chopping et al., 2003; Urso et al., 2004; Veroustraete and Verstraiten, 2004), but few have addressed directly the value for damage assessment and mapping of discolouration. The spectral band of the forward stereo channel (directed 35° off-nadir) of the spruce budworm stereo filter set was designed to be the same as one of the nadir channels and be in a spectral band (near-infrared) that is good for discriminating discolouration levels. However, several factors may have reduced this channel's effectiveness in classifications of discolouration in this study and decreased its contribution to class separability (J–M distance) for band combinations. The original resolution for the forward looking channel was slightly less than that of the nadir bands, forward looking data are acquired at different times and aircraft positions and thus interband registration with the nadir bands may not be as good as among the nadir bands themselves, and flight direction and sun azimuth were such that the stereo channel was viewing the side of the trees that was partly self shaded.

When compared to the 780 nm nadir band, the 780 nm forward looking channel was not any better for differentiating discolouration levels. The single band J–M distance was somewhat lower averaged over four discolouration classes (nil-trace, light, moderate and severe) and slightly higher averaged over the light, moderate and severe classes. The regression analysis showed the stereo channel to be poorer for discriminating discolouration levels. There was no advantage in adding the stereo channel to a six band classification or substituting it for the nadir band. Based on this study there does not seem to be any advantage in having oblique viewing spectral bands, but additional testing is in order.

5. Conclusions

Specialized spectral bands designed for detection of the red colouration of current budworm defoliation worked well for classifying jack pine budworm discolouration. Only three or four well-placed spectral bands are needed for a good classification. Accurate classification (84%) of four levels of discolouration was achieved. The portrayal of discolouration was useful at the stand level as well as for patterns within stands. Simple operationally feasible multispectral imagery and techniques are appropriate. Resolutions in the order of 2.5 m were sufficient, single tree analysis was not necessary. Although hyperspectral data and analysis was not needed, the ability of such sensors to acquire data in the appropriate narrow bands makes them suitable for such applications. Therefore, information from such automated techniques can provide useful input for mapping and monitoring discolouration (current year defoliation), jack pine budworm decision support systems, forest inventory, harvest scheduling, salvage logging and planning budworm control programs and thus can help with determining forest management options.

Acknowledgements

Dr. Larry Marshall formerly of the Canadian Forest Service is thanked for helping initiate the study. S. Payne of the Forest Insect and Disease Survey (CFS) conducted a special defoliation survey for the study. Innotech Aviation Enterprises Ltd. flew, processed and geometrically corrected the MEIS data. Max Buchheit and Dr. Jack Gibson with the Canada Centre for Remote Sensing (CCRS) assisted with aspects of the geometric correction. CCRS and in particular Dr. Bob Neville were instrumental in getting the specialized spectral filter set manufactured, tested and installed. Dr. Vince Nealis, Joan Luther, both of the CFS and Dr. Peter Murtha of the University of British Columbia provided useful comments on the manuscript. Dr. Ron Hall (CFS) contributed to the study and manuscript review and Sally Tinis and David Hill of the Canadian Forest Service assisted with aspects of the final stages of the study.

References

Ahern, F.J., Sirois, J., McColl, W.D., Gauthier, R.P., Alföldi, T.T., Patterson, W.H., Erdle, T.A., 1991. Progress toward improving aerial defoliation survey methods by using electronic imagers. Photogramm. Eng. Remote Sens. 57, 187–193.

Aldrich, R.C., Heller, R.C., Bailey, W.P., 1958. Observation limits for aerial sketch-mapping southern pine beetle damage in the southern Appalachians. J. For. 56, 200–202.

Alfaro, R.I., 1991. Damage assessment and integrated pest management of forest defoliators. For. Ecol. Manage. 39, 275–281.

British National Space Centre (BNSC), 2002. New low cost UK earth observation instrument orbits the earth on a European satellite. URL (last accessed 29/11/2004): http://www.bnsc.gov.uk/default.aspx%3F;nid=3420%26;hl=chris.

Canadian Forest Service, 2002. The State of Canada's Forests 2001–2002. Canadian Forest Service, Natural Resources Canada, Ottawa, Ontario, 63 pp.

Cerezke, H.F., 1986. Impact studies of jack pine budworm, *Choristoneura pinus pinus*, in Nisbet Provincial Forest, Saskatchewan. In: Jack Pine Budworm Information Exchange, Manitoba Natural Resources, Winnipeg, Manitoba, pp. 25–38.

Chen, J.M., Leblanc, S.G., 1997. A four-scale bidirectional reflectance model based on canopy architecture. IEEE Trans. Geosci. Remote Sens. 35, 1316–1337.

Chen, G.M., Liu, J., Leblanc, S.G., Laxaze, R., Roujean, J.L., 2002. Multi-angular optical remote sensing for assessing vegetation structure and carbon absorption. Remote Sens. Environ. 84, 515–525.

Chopping, M.J., Rango, A., Havstad, K.M., Schiebe, F.R., Ritchie, J.C., Schmugge, T.J., French, A.N., Su, L., McKee, L., Davis, M.R., 2003. Canopy attributes of desert grassland and transition communities derived from multiangular airborne imagery. Remote Sens. Environ. 85, 339–354.

Ciesla, W.M., 2000. Remote Sensing in Forest Health. Forest Health Technology Enterprise Team Report No. 00-03. USDA Forest Service, Fort Collins, CO, 266 pp.

Coops, N., Stanford, M., Old, K., Dudzinski, M., Culvenor, D., Stone, C., 2003. Assessment of dothistroma needle blight of Pinus radiata using airborne hyperspectral imagery. Phytopatholagy 93, 1524–1532.

Danson, F.M., Curran, P.J., 1991. Structural controls on remotely sensed response of a coniferous forest plantation. In: Proceedings of the Fifth Physical Measurements and Signatures in Remote Sensing, Courcheval, France, pp. 606–609.

Deschamps, P.Y., Bréon, F.M., Leroy, M., Podaire, A., Bricaud, A., Buriez, J.C., S'eze, G., 1994. The POLDER mission: instrument characteristics and scientific objectives. IEEE Trans. Geosci. Remote Sens. 32 (3), 598–615.

Diner, D.J., Asner, G.P., Davies, R., Knyazikhin, Y., Muller, J.-P., Nolin, A.W., Pinty, B., Schaaf, C.B., Stroeve, J., 1998a. The Airborne Multi-angle Imaging SpectroRadiometer (AirMISR): instrument description and first results. IEEE Trans. Geosci. Remote Sens. 36, 1339–1349.

Diner, D.J., Asner, G.P., Davies, R., Knyazikhin, Y., Muller, J.-P., Nolin, A.W., Pinty, B., Schaaf, C.B., Stroeve, J., 1998b. Multiangle Imaging SpectoRadiometer (MISR) instrument description and experimental overview. IEEE Trans. Geosci. Remote Sens. 36, 1072–1087.

Diner, D.J., Asner, G.P., Davies, R., Knyazikhin, Y., Muller, J.-P., Nolin, A.W., Pinty, B., Schaaf, C.B., Stroeve, J., 1999. New directions in earth observing: scientific applications of multiangle remote sensing. Bull. Am. Meteorol. Soc. 80 (11), 2209–2228.

Ekstrand, S.P., 1990. Detection of moderate damage on Norway spruce using Landsat TM and digital stand data. IEEE Trans. Geosci. Remote Sens. 28, 685–692.

Ekstrand, S.P., 1994. Assessment of forest damage with Landsat TM: correction for varying forest stand characteristics. Remote Sens. Environ. 47, 291–302.

Forest Insect and Disease Survey, 1980–1995. Forest insect and disease conditions in Canada 1995. In a series of reports dated 1980 through 1995. Forest Insect and Disease Survey, Canadian Forest Service, Natural Resources Canada, Ottawa, Ontario.

Franklin, S.E., 1989. Classification of hemlock looper defoliation using Spot HRV imagery. Can. J. Remote Sens. 15, 178–182.

Franklin, S.E., Waring, R.H., McCreight, R.W., Cohen, W.B., Fiorella, M., 1995. Aerial and satellite sensor detection and classification of Western Spruce Budworm defoliation in a subalpine forest. Can. J. Remote Sens. 21, 1–32.

Franklin, S.E., Wulder, M.A., Skakun, R.S., Carol, A.L., 2003. Mountain pine beetle red-attack forest damage classification using stratified Landsat TM data in British Columbia, Canada. Photogramm. Eng. Remote Sens. 69, 283–288.

Gastellu-Etchegorry, J.P., Martin, E., Gascon, F., 2004. DART: a 3D model for simulating satellite images and studying surface radiation budget. Int. J. Remote Sens. 25, 73–96.

Gemmel, F., McDonald, J., 2000. View zenith angle effects on the forest information content of three spectral indices. Remote Sens. Environ. 72, 139–158.

Gibson, J.R., Buchheit, M., Hak, L., 1994. Geometric correction and terrain height extraction using stereo electro-optical digital imagery. In: Proceedings of the First International Airborne Remote Sensing Conference and Exhibition, vol. II, Strasbourg, France, pp. 412–423.

Hall, F.G., Peddle, D.R., LeDrew, E.F., 1996. Remote sensing of biophysical variables in boreal forest stands of *Picea mariana*. Int. J. Remote Sens. 17, 3077–3081.

Hall, R.J., Crown, P.H., Titus, S.J., Volney, W.J.A., 1995a. Evaluation of Landsat Thematic Mapper data for mapping top kill caused by jack pine budworm defoliation. Can. J. Remote Sens. 21, 388–399.

Hall, R.J., Volney, W.J.A., Knowles, K., 1995b. Hazard rating and stand vulnerability to jack pine budworm defoliation using GIS. In: Volney, W.J.A., Nealis, V.G., Howse, G.M., Westwood, A.R., McCullough, D.R., Laishley, B.L. (Eds.), Jack Pine Budworm Biology and Management. Information Report NOR-X-342. Natural Resources Canada, Canadian Forest Service, Edmonton, Alberta, pp. 121–132.

Harris, J.W.E., Dawson, A.F., 1979. Evaluation of Aerial Forest Pest Damage Survey Techniques in British Columbia. Information Report BC-X-198. Pacific Forest Research Centre, Canadian Forest Service, Victoria, BC, 13 pp.

Heller, R.C., Coyne, J.F., Bean, J.L., 1955. Airplanes increase effectiveness of southern beetle surveys. J. For. 53, 483–487.

Hopkins, P.F., MacLean, A.L., Lillesand, T.M., 1988. Assessment of Thematic Mapper imagery for forestry applications under Lake States conditions. Photogramm. Eng. Remote Sens. 54, 61–68.

Howse, G.M., Meating, J.H., 1995. Jack pine budworm situation in Ontario 1981–1994. In: Volney, W.J.A., Nealis, V.G., Howse, G.M., Westwood, A.R., McCullough. D.R., Laishley, B.L. (Eds.), Jack Pine Budworm Biology and Management. Information Report NOR-X-342. Natural Resources Canada, Canadian Forest Service, Edmonton, Alberta, pp. 31–34.

Irons, J.R., Ranson, K.J., Williams, D.L., Irish, R.R., Huegel, F.G., 1991. An off-nadir-pointing imaging spetroradiometer for terrestrial ecosystem studies. IEEE Trans. Geosci. Remote Sens. 29, 66–74.

Knapp, A., Hoppus, M., 1996. Evaluation of a color infrared digital camera system for forest health protection applications. In: Proceedings of the Sixth Forest Service Remote Sensing Applications Conference, Denver, CO, pp. 213–219.

Lawrence, R., Labus, M., 2003. Early detection of Douglas-fir beetle infestation with subcanopy resolution hyperspectral imagery. West. J. Appl. For. 18, 202–206.

Leckie, D.G., 1987. Factors affecting defoliation assessment using airborne multispectral scanner data. Photogramm. Eng. Remote Sens. 53, 1665–1674.

Leckie, D.G., Gougeon, F.A., 1981. Assessment of spruce budworm defoliation using digital airborne MSS data. In: Proceedings of the Seventh Canadian Symposium on Remote Sensing, Winnipeg, Manitoba, pp. 190–196.

Leckie, D.G., Kneppeck, I.D., 1986. A trial of oblique imagery from a low cost video camera system for defoliation assessment. In: Proceedings of the 10th Canadian Symposium on Remote Sensing, Edmonton, Alberta, pp. 919–926.

Leckie, D.G., Ostaff, D.P., 1988. Classification of airborne multispectral scanner data for mapping current defoliation caused by the spruce budworm. For. Sci. 34, 259–275.

Leckie, D.G., Teillet, P.M., Ostaff, D.P., Fedosjevs, G., 1988. Sensor band selection for detecting current defoliation caused by the spruce budworm. Remote Sens. Environ. 26, 31–50.

Leckie, D.G., Ostaff, D.P., Teillet, P.M., Fedosjevs, G., 1989. Spectral characteristics of tree components of balsam fir and spruce damaged by spruce budworm. For. Sci. 35, 582–600.

Leckie, D.G., Beaubien, J., Gibson, J.R., O'Neill, N.T., Piekutowski, T., Joyce, S.P., 1996. Data processing and analysis for MIFUCAM: a trial of MEIS imagery for forest inventory mapping. Can. J. Remote Sens. 21, 337–356.

Leckie, D.G., Jay, C., Gougeon, F.A., Sturrock, R.N., Paradine, D., 2004. Detection and assessment of trees with *Phellinus weirii* laminated root rot using high resolution multi-spectral imagery. Int. J. Remote Sens. 25, 793–818.

Leroy, M., Bréon, F.-M., 1996. Angular signatures of surface reflectances from airborne POLDER data. Remote Sens. Environ. 57, 97–107.

Luther, J., Franklin, S.E., Hudak, J., 1991. Satellite remote sensing of current year defoliation by forest pests in western Newfoundland. In: Proceedings of the 14th Canadian Symposium on Remote Sensing, Calgary, Alberta, pp. 192–198.

MacLean, D.A., 1990. Impact of forest pests and fire on growth and timber yield: implications for forest management planning. Can. J. For. Res. 20, 391–404.

MacLean, D.A., MacKinnon, W., 1996. Accuracy of aerial sketch mapping estimates of defoliation. Can. J. For. Res. 26, 2099–2108.

MacLean, D.A., Coulson, R., 2001. Why aren't more decision support systems for insect management actually being used? In: Volney, W.J.A., Spence, J.R., Lefebvre, E.M. (Eds.), Boreal Odyssey—Proceedings of the North American Forest Insect Work Conference. Information Report NOR-X-381. Natural Resources Canada, Canadian Forest Service, Northern Forestry Centre, Edmonton, Alberta, pp. 159–161.

McColl, W.D., Neville, R.A., Till, S.M., 1984. Multidetector electro-optical imaging sensor MEIS II. In: Proceedings of the Eighth Canadian Symposium on Remote Sensing, Montreal, Quebec, pp. 71–79.

McConnell, T.J., 1994. Proceedings Aerial Pest Detection and Monitoring Workshop. Los Vegas, Nevada. Report 95-4, USDA Forest Service, Northern Region Pest Management Missoula, MT, 103 pp.

McCullough, D.G., Marshall, L.D., 1993. Jack pine budworm decision support system: a case study. Compiler 11, 14–20.

McCullough, D.G., 2000. A review of factors affecting the population dynamics of jack pine budworm (*Choristonuera pinus pinus* Freeman). Popul. Ecol. 42, 243–256.

Moody, B.H., 1986. The jack pine budworm history of outbreaks, damage and FIDS sampling and prediction system in the prairie provinces. In: Jack Pine Budworm Information Exchange, Manitoba Natural Resources, Winnipeg, Manitoba, 15–22.

Murtha, P.A., Bortolot, Z., Thurston, J., 2000. A Landsat TM spectral unmixing mountain pine beetle attack-fraction probability map in the Vanderhoof forest district, British Columbia. In: Proceedings of the 22nd Canadian Symposium on Remote Sensing, Victoria, BC, pp. 445–450.

Myhre, R.J., Graham, L.A., Sumpter, C.W., 1990. Airborne video. In: Proceedings of the Third Forest Service Remote Sensing Applications Conference, Denver, CO, pp. 293–298.

Nealis, V.G., Magnussen, S., Hopkin, A.A., 2003. A lagged, density-dependent relationship between jack pine budworm *Choristoneura pinus pinus* and its host tree *Pinus banksiana*. Ecol. Entomol. 28, 183–192.

Power, J.M., Gillis, T., 1995. Decision support tools for jack pine budworm management—progress and plans. In: Volney, W.J.A., Nealis, V.G., Howse, G.M., Westwood, A.R., McCullough, D.R., Laishley, B.L. (Eds.), Jack Pine Budworm Biology and Management. Information Report NOR-X-342. Natural Resources Canada, Canadian Forest Service, Edmonton, Alberta, pp. 133–141.

Radeloff, V.C., Mladenoff, D.J., Boyce, M.S., 1999. Detecting jack pine budworm defoliation using spectral mixture analysis: separating effects from determinants. Remote Sens. Environ. 69, 156–169.

Reinartz, P., Müller, R., Kritikos, G., 1988. Neue Ansätze zur Opimierung der Klassifizierung von Wald- und Waldschadensdaten. Deutsche Forschungs- und Versuchsanstalt für Luft- und Raumfarht. Oberpfaffenhofen, Germany, 60 pp.

Richards, J.A., 1993. Remote Sensing Digital Image Analysis, second ed. Springer-Verlag, New York, 240 pp.

Rowe, J.S., 1972. Forest Regions of Canada. Publication No. 1300. Canadian Forest Service, Ottawa, Ontario.

Sakun, R.S., Wulder, M.A., Franklin, S.E., 2003. Sensitivity of the thematic mapper enhanced wetness difference index to detect mountain pine beetle red-attack damage. Remote Sens. Environ. 86, 433–443.

Sandau, R., Braunecker, B., Driescher, H., Eckardt, A., Hilbert, S., Hutton, J., Kirchhofer, W., Lithopoulos, E., Reulke, R., Wicki, S., 2000. Design principles of the LH Systems ADS40 Airborne Digital Sensor. In: International Archives Photogrammetry and Remote Sensing, Part B1, vol. 33, Amsterdam, Netherlands, pp. 258–265.

Stenberg, P., Nilson, T., Smolander, H., Voipio, P., 2003. Gap fraction estimation of LAI in Scots pine stands subjected to experimental removal of branches and stems. Can. J. Remote Sens. 29, 363–370.

Tian, Y.H., Wang, Y.J., Zhang, Y., Knayazikhn, Y., Bogaert, J., Myneni, R.B., 2003. Radiatiove transfer based scaling of LAI retrievals from reflectance data of different resolutions. Remote Sens. Environ. 87, 143–159.

Urso, G.D., Dini, L., Vuolo, F., Alonso, L., Guanter, L., 2004. Retrieval of leaf area index by inverting hyper-spectral, multi-angular CHRIS/Proba data from SPARC 2003. In: Proceedings of the Second CHRIS/PROBA Workshop (ESA SP-578). Frascati, Italy. URL (last visited 29/10/2004) http://earth.esa.int/workshops/chris_proba_04/papers/15_durso.pdf.

Verhoef, W., Bach, H., 2003. Simulation of hyperspectral and directional radiance images using coupled biophysical and atmospheric radiative transfer models. Remote Sens. Environ. 87, 23–41.

Veroustraete, F., Verstraiten, W.W., 2004. Extraction of biophysical variables using VGT-P multi-angular observations: preliminary results. In: Second International VEGETATION Users Conference (Section II). Antwerp, Belgium. URL (last visited 29/10/2004): http://www.vgt.vito.be/vgtapen/pages/fullpapers/Veroustraete_full.PDF.

Volney, W.J.A., 1988. Analysis of historic jack pine budworm outbreaks in the Prairie provinces of Canada. Can. J. For. Res. 18, 1152–1158.

Volney, W.J.A, Nealis, V.G., Howse, G.M., Westwood, A.R., McCullough, D.R., Laishley, R.L. (Eds.), 1995. Jack Pine Budworm Biology and Management. Information Report NOR-X-342. Natural Resources Canada, Canadian Forest Service, Edmonton, Alberta, 158 pp.

Wang, Y.J., Buermann, W., Stenberg, P., Smolander, H., Hame, T., Tian, Y.H., Hu, J.N., Knyazikhn, Y., Myneni, R.B., 2003. A new parameterization of canopy spectral response to incident solar radiation: case study with hyperspectral data from pine dominant forest. Remote Sens. Environ. 85, 304–315.

Waters, W.E., Heller, R.C., Bean, J.L., 1958. Aerial appraisal of damage by the spruce budworm. J. For. 56, 269–276.

Wehn, H., Goldstein, N., Ameri, B., Moshkovitz, A., Zwick, H., 2002. Frequent-Image-Frames Enhanced Digital Ortho-Rectified Mapping (FIFEDOM) airborne mapping system. In: International Geoscience Remote Sensing Symposium 2002, Toronto, Canada, pp. 1296–1299.

Wert, S.L., Roettgering, B., 1967. Aerial Survey of Insect Caused Mortality—Operation Recorder Gathers Data Quickly, Cheaply. Research Note PSW-150. Pacific Southwest Forest and Range Experiment Station, USDA Forest Service, Berkeley, CA.
Zarco-Tejada, P.J., Miller, J.R., Mohammed, G.H., Noland, T.L., Sampson, P.H., 2002. Vegetation stress detection through chlorophyll a + b estimation and fluorescence effects on hyperspectral imagery. J. Environ. Qual. 31, 1433–1441.
Zwick, H.H., McColl, W.D., Edel, H.R., 1980. The CCRS DS1260 Airborne Multispectral Scanner (MSS). In: Proceedings of the Seventh Canadian Symposium on Remote Sensing, Halifax, NS, pp. 643–648.